Journal of Plant Growth Regulation (2019) 38:1354–1361
https://doi.org/10.1007/s00344-019-09938-5

Characterization of Top Leader Elongation in Nordmann Fir (*Abies nordmanniana*)

Helle Juel Martens[1] · Steen Sørensen[2] · Meike Burow[3] · Bjarke Veierskov[1]

Received: 6 September 2018 / Accepted: 21 January 2019 / Published online: 13 March 2019

Abstract
Our understanding of the developmental changes that occur during top leader elongation in gymnosperms lags behind that in angiosperms. We developed a semiquantitative method for determining epidermal cell size, by measuring the Feret diameter after cell wall staining of stem epidermal peels. This method allowed a large number of cells to be measured at various locations in the top leader of the Christmas tree *Abies nordmanniana*. Further, we have identified the growth rate of individual sections of the top leader, and the relationship between cell length and needle arrangement throughout the top leader. At bud break, all stem units begin to elongate simultaneously, but growth ceases from the base upwards during top leader elongation. Long top leaders were characterized by having up to three times as long cells at the base compared to short top leaders, whereas the cell lengths were similar in the apical region independent of the given plant growth capacity. In the basal sector, the level of auxin was much higher, whereas the levels of cytokinins were lower than in the apical sector, causing the auxin/cytokinin ratio to change from about 3 in the apical sector to more than 20 in the basal part. The Fibonacci number changed in the apical sector due to an increased cell number in the stem units and therefore longer distance between the needles. We conclude that the general growth pattern during top leader elongation in *A. nordmanniana* is similar to angiosperms but differs at the cellular level.

Keywords Auxin · Cytokinin · Stem elongation · Feret diameter

Introduction

Conifers belong to an ancient group of seed plants that differ from angiosperms at the physiological and morphological level (Chen et al. 1996; Liesche et al. 2011; Tillman-Sutela and Kauppi 2000). In conifers, the yearly growth cycle is spread over two growing seasons, in the sense that a non-elongating shoot initial is formed within the apical meristem each year, but the elongation thereof does not occur until the following year (Chen et al. 1996; Hejnowicz and Obarska 1995). In angiosperms, these two processes occur simultaneously during the growth season.

The fundamental shape of a plant is predetermined by its meristems, yet its final size is controlled by coordinated cell division and elongation processes (Willis et al. 2016). The development of the shoot apical meristem (SAM) in angiosperms is well documented (Willis et al. 2016), whereas the knowledge of these processes in gymnosperms is more limited. In angiosperms, stem cells are located in the central zone at the very tip, whereas the peripheral zone consists of the epidermal (L1) and subepidermal (L2) layers. The size of the meristem is regulated by cytokinins by controlling the pool of undetermined cells in the apical meristem and brassinosteroids that maintain the meristematic boundaries between SAM and the epidermal L1 layer (Savaldi-Goldstein et al. 2007; Zadnikova and Simon 2014). Auxin accumulation in the L1 layer is regulated by the PIN1 auxin efflux carrier whereby location of the leaf initials is controlled and thus the phyllotaxis of the shoot. Whether this is also the case in gymnosperms is yet to be uncovered. Petals, sections,

✉ Bjarke Veierskov
bv@plen.ku.dk

Steen Sørensen
shs@pc.dk

[1] Department of Plant and Environmental Sciences, Transport Biology, University of Copenhagen, Thorvaldsensvej 40, 1871 Frederiksberg C, Denmark

[2] Steen Sørensen Aps, Pøelvej 8, 8340 Malling, Denmark

[3] DynaMo Center, Department of Plant and Environmental Sciences, University of Copenhagen, Thorvaldsensvej 40, 1871 Frederiksberg C, Denmark

seeds or leaves are often arranged in a spiral arrangement around a stem, and this arrangement can be described by the Fibonacci number (a sequence of numbers where each number is the total of the previous two numbers added together). The basis for the spiral development is asymmetric cell divisions in the meristems. This occurs as one of the newly divided cells begins maturation, whereas the other continues to divide. The spiral growth comes about if the cell division time differs from the maturation time (Boman et al. 2017; Brousseau 1969). The Fibonacci number remains constant as long as the relationship between cell division and maturation time remains constant (Boman et al. 2017). In conifers, it is generally accepted that the needle phyllotaxis is predetermined in the primordial first-year shoot (Sutinen et al. 2009). The Fibonacci number may thus reflect the developmental stability within the meristem during the time of development.

After bud break, the driving force for internode elongation originates from the internal turgor pressure, primarily the pith cells, whereas the epidermal cells restrict growth (Kutschera and Nikas 2007). In the young angiosperm internodes, cell division is maintained by a low auxin/cytokinin ratio, but it ceases at the time when the maximum rate of internode elongation is observed. From then on, further growth only occurs as cell elongation (Maksymowych et al. 1989). Stem growth in angiosperms is thus an ongoing process that continues over several nodes, but changes character as the distance from the apical meristem increases.

In the shoot of most conifers such as spruce, pine and fir, needle insertions into the top leader generally lack axillary buds (Veierskov et al. 2008). Thus, the terms node and internode are not applicable terms for these plants; instead, the term stem unit is used. When annual growth is initiated, the stem units throughout the primordial shoot begin to elongate at the same time (Baxter and Cannell 1978). However, to reach the final size, additional cell divisions most likely occur within the stem units (Hejnowicz and Obarska 1995). The goal of the present paper is to answer the question whether growth of the top leader of Nordmann fir occurs by the simultaneous elongation of all stem units throughout the growth period, or by a gradual, basipetal elongation as in angiosperms and further to determine whether cell division and maturation within the stem units are stable throughout the development of the top leader.

Materials and Methods

The plant material originated from 8-year *Abies nordmanniana* Spach prov. Ambrolauri trees grown at a commercial Christmas tree farmer in Malling, Denmark as described by (Rasmussen et al. 2003). The plants were grown under ambient weather conditions. Top leaders were collected from the growing seasons 2014 and 2015.

Growth Determinations

On June 28, 2014, 40 plants with a top leader length of 125 mm were selected. The top leaders of these plants were divided into three equal sections (apical, middle or basal sector, Fig. 1) by ink marks, and the length of each section was monitored weekly until September 1. Needle distance was then measured with a vernier caliper on the top leaders.

On June 3rd 2015, 100 plants of similar developmental stage were selected. On July 15, the length of the top leaders was determined, and the plants grouped according to length. Five top leaders from each of the groups, short (approx. 90 mm), medium (approx. 130 mm) and long (approx. 270 mm) were selected.

Each top leader was divided into five sample points for epidermis cell length determinations (Fig. 1). The size of the epidermal cells was measured at the apical and basal part of each top leader for a total of approx. 700 cells for each top leader, as described under quantitative microscopy. Epidermis sections from sample point 5 within a long top leader were fixed and stained with 4,6-diamino-phenylindole (DAPI) for visualization of mitotic activity (Powikrowska et al. 2014).

On July 15, five top leaders from the groups 90 mm or 270 mm long were harvested for hormone determination. From each size group, 10 mm sections from sample point 1 and 5 were excised, pooled and immediately frozen in liquid nitrogen and kept at − 80 °C until used for hormone analysis as described by (Rasmussen et al. 2009).

Growth-Regulated Plants

On June 25, 2014, growth season, 40 top leaders approximately 15 cm long were treated with 2 ml of a 1.5% solution (80 mM) Pomoxon ® (NAA, 1-Naphthalene acetic acid) with an Easy Roller System as described by (Rutledge et al. 2009). On July 7, the top leaders were treated a second time according to standard growth regulating procedures used by commercial Christmas tree growers. On August 18, when top leader elongation had ceased, top leaders from 3 NAA treated and 3 untreated plants were harvested. The top leaders of these plants were divided into 5 sample points (see Fig. 1), and needle arrangement was determined in each of these sample points. Cell length was determined for each plant for approximately 50 epidermis cells from the top (sample point 1) and for base (sample point 5) as described under quantitative microscopy.

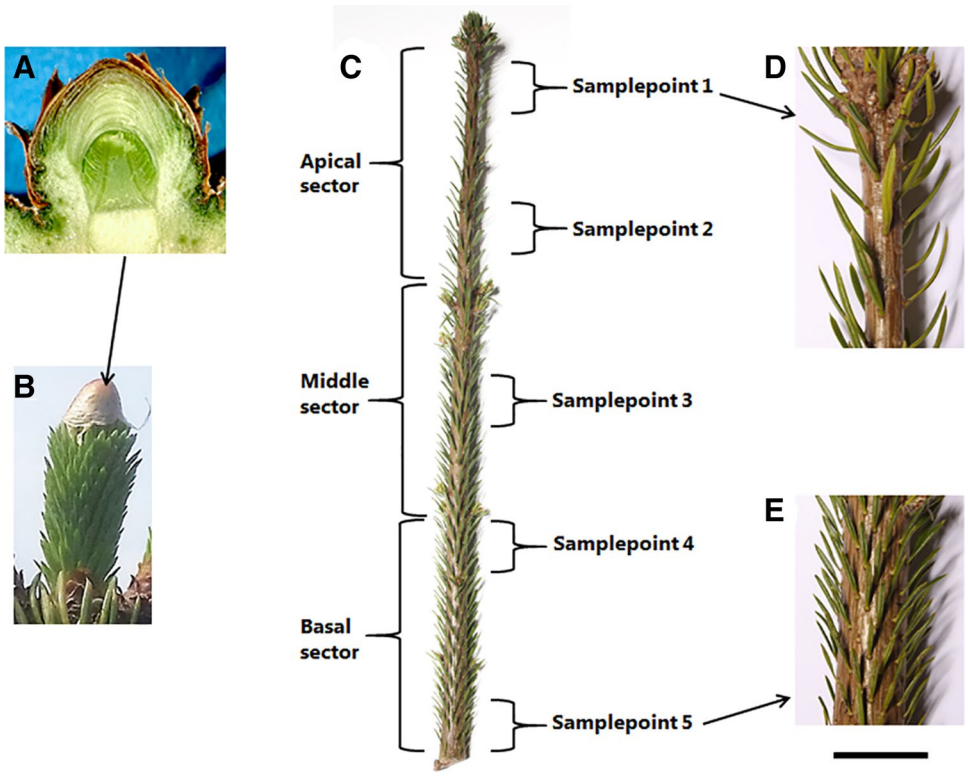

Fig. 1 Morphological characterization of an *A. nordmanniana* top leader. A: apical bud before bud break. B: the expanding top leader after bud break. C: the 270-mm-long top leader divided into 3 sectors for determination of growth rates, and into 5 sample points for determination of cell size and hormone composition. D: needle distribution at sample point 1. E: needle distribution at sample point 5. Bar = 10 mm

Quantitative Microscopy

Epidermis areas, 1 × 0.5 cm, were peeled off with a fine forceps from the basal part of the shoot (sample point 5) and the tip part (sample point 1) just below the bud. Epidermis peels were fixed for 15 min in glutaraldehyde–formaldehyde solution and stained with the fluorescent dye Coriphosphine O for visualization of cell walls. Images were recorded in a Nikon DM fluorescence microscope at 10× magnification using a UV excitation filter (380–420 nm) with LP450 emission and analyzed using Image J software (https://imagej.nih.gov/ij/, 1997–2016). A semi-automated analysis was devised for measuring the maximum Feret diameter. Images were obtained with a digital camera and converted into binary format with ImageJ. The following commands were used for the conversion;:grey mode, threshold and watershed. Due to dense cytoplasm in the top sector cells, the cell interior was manually separated from cell wall outline in some images. This operation was performed after thresholding not interfering with image interpretation. The $Feret_{max}$ diameter (termed Feret diameter in the text) from the total number of intact cells was then obtained with the analyse command. The images were converted into binary representations and analyzed to determine the Feret diameter of individual cells. The image analysis method was accurate as seen by overlaying the binary outlined image onto the original (data not shown). The results were directly loaded into Excel spreadsheet program for analysis.

Phytohormone Analysis

Phytohormones were extracted from around 200 mg (FW) plant material ground in liquid nitrogen with 1.25 ml 85% (v/v) methanol containing 4 µl of internal standard mix containing 88 pmol (2H5)tZ and 216 pmol (2H6)ABA. Samples were thoroughly vortexed, incubated for 30 min at 4 °C, and centrifuged (20,000*g*, 4 °C, 15 min). Supernatants were passed through C18 columns (Chromafix, Macherey–Nagel, Düren/Germany) after pre-equilibration with three times 3 ml 80% (v/v) methanol and flow-throughs were collected and kept on ice. Extraction was repeated with 1.25 ml 85% (v/v) methanol, and second extracts were passed through the same columns. The combined extracts were concentrated using a SpeedVac. The residues were dissolved in 1 ml 20% (v/v) methanol by brief sonication and filtered (MultiScreenHTS; EMD Millipore, cat no. MSGVN 2250). Phytohormones were analyzed by UHPLC/TQ-MS on an AdvanceTM-UHPLC/EVOQTMElite-TQ-MS instrument (Bruker) equipped with a C-18 reversed phase column (Kinetex 1.7 u XB-C18, 10 cm × 2.1 mm, 1.7 µm particle size, Phenomenex) by using a 0.05% formic acid in water (v/v), pH 4.0 (solvent A)–methanol (solvent B) gradient at a flow rate of 0.4 ml/min at 40 °C. The gradient applied was as follows: 10–50% B (15 min), 50% (2 min), 50–100% B (0.1 min), 100% B (2.9 min), 100–10% B (0.1 min), and 10% B (5 min). Compounds were ionized by ESI with a spray voltage of + 4500 V and − 4000 V in positive and

negative mode, respectively, heated probe temperature 350 °C, cone temperature 300 °C. Quantification was based on response factors relative to ($^2H_5$)*trans*-zeatin (positive mode) and ($^2H_6$)abscisic acid (negative mode). The individual hormones were monitored based on the following MRM transitions: ($^2H_5$)*trans*-zeatin, (+) 225 > 137 [15 V]; ($^2H_6$)abscisic acid, () 269 > 159 [7 V]; dihydrozeatin, (+) 222 > 136 [15 V]; indole-acetic acid, (+) 176 > 130 [10 V]; N^6-Δ^2-(isopentenyl)adenine, (+) 204 > 136 [10 V]; tZ, (+) 220 > 136 [15 V]; *trans*-zeatin riboside, (+) 352 > 220 [15 V]; *trans*-zeatinriboside-*O*-glucoside, (+) 514 > 382 [15 V].

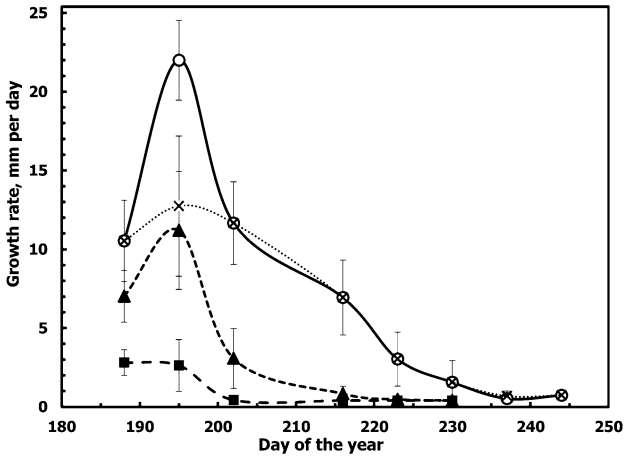

Fig. 2 Stem elongation of the top leader of *A. nordmanniana* during the growth season. Top leaders with a length of 125 mm were divided into 3 sectors at June 28th 2014 (day 188). The daily growth was determined until September 1 for each sector (filled square: basal sector; filled triangle: middle sector; times: apical sector) and the entire top leader (open circle). N = 40 of different top leaders; values give mean ± SD

Results

In *A. nordmanniana*, a complete shoot initial is present within the bud, and at budburst all the needle initials appear simultaneously (Fig. 1A, B). However, during the top leader elongation, needle distance becomes uneven (Fig. 1D, E). Not only the needle distance varied between the base and top of the top leader (Fig. 1; Table 2), but so did the daily growth rate. At the base, the fastest growth rate was 2.4 mm per day obtained July 7, and the growth stopped by July 21. In the middle and top sections, the growth rate peaked July 14 at a rate of 10.8 and 21.6 mm per day, respectively. However, whereas the growth at the middle section had ceased by August 11, growth continued in the top section until early September (Fig. 2). Determining the length of the epidermis cells revealed that the cells at the basal sample point 5 were longer than the cells at the apical sample point 1 (Fig. 3), and a long top leader coincided with longer cells at basal sample point 1. The same was observed in the apical sample point, but only as a tendency (Fig. 5). For image analysis, operator

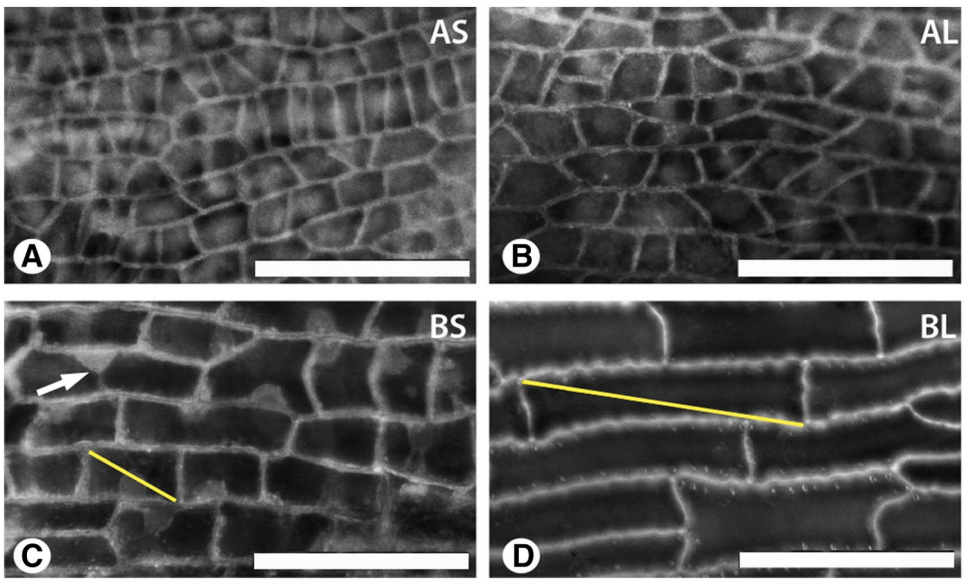

Fig. 3 Grey-level images of *A. nordmanniana* stem epidermis peels after staining with coriphosphine. **a, b** Cells from the apical sector of a short and a long top leaders, respectively. **c, d** Cells from the basal sector of a short top leader and a long top leader, respectively. The yellow lines show examples of Feret diameter (**c, d**). Note that cytoplasm and nucleus (arrow) are visible in the epidermis from short stem (**c**). AS and AL: sample point 1 within the apical sector of short (90 mm) and long (270 mm) top leaders. BS and BL: sample point 5 within the basal sector of short (90 mm) and long (270 mm) top leaders. Bar = 100 µm. (Color figure online)

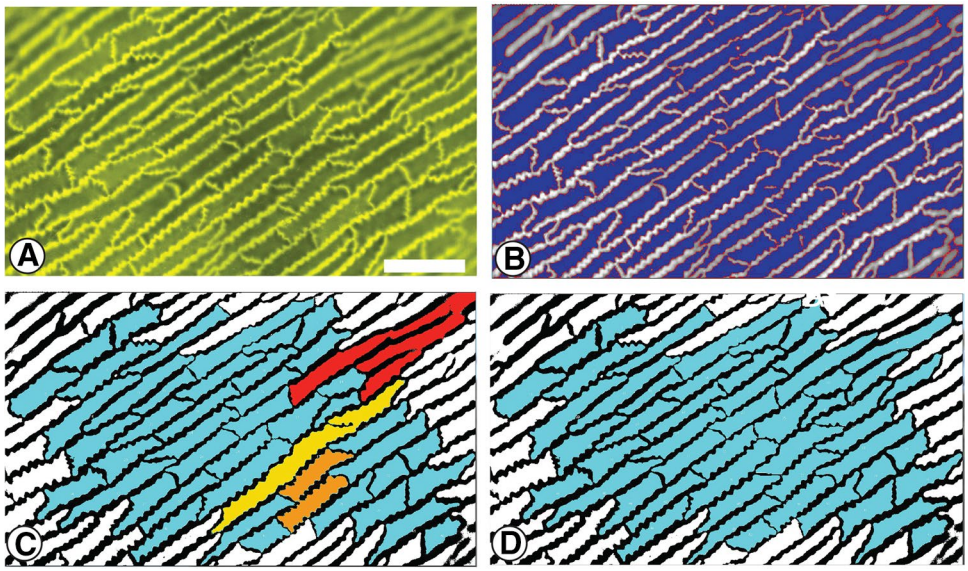

Fig. 4 Semiautomatic image analysis of epidermis cell dimensions from *A. nordmanniana* top leaders sampled in the elongation period. The original fluorescence image from sample point 5 within a basal sector of a long top leader (**a**) was converted into a grey-level image and segmented into cell lumen (**b**). In the case of discontinuous cell wall outlines, as seen in the red, orange and yellow areas (**c**), these were adjusted manually. The epidermis cells were analyzed while excluding incomplete cells at image edges (**d**). Bar = 100 µm. (Color figure online)

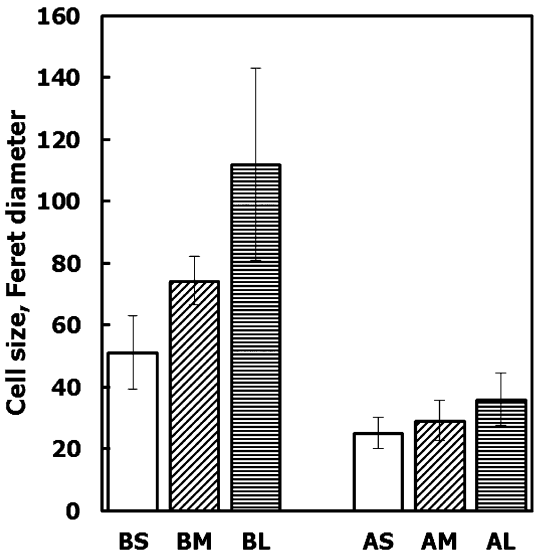

Fig. 5 Relationship between the length of top leaders in *A. nordmanniana* and the size of epidermis cells. Cell size was determined as Feret diameter. Each value is the average of minimum 350 cell measurements from 3 individual plants harvested in June 2015. A: sample point 1 within the apical sector, B: sample point 5 within the basal sector, S: short top leaders (90 mm), M: medium top leaders (130 mm), L: long top leaders (270 mm). Bars denote 95% confident limits

intervention was necessary wherever nuclei and cytoplasmic strands had similar fluorescence intensity levels as the cell walls (Fig. 3c), or if the cells were small with dense cytoplasm (Fig. 3a), or to separate erroneously joined cells (Fig. 4c). Detailed studies of the distribution of the length of epidermal cells in short, medium and long top leaders showed that in short top leaders the distribution in all three sectors was very narrow (between 10 and 60 µm), whereas in the basal sector of medium and long top leaders a huge variation in cell length was determined (between 25 and 260 µm, Fig. 6). Hormonal analysis showed that the auxin level was much higher in the basal sample points compared to the apical sample point independent of the length of the top leader (270% and 143% in short and long top leaders, respectively). In the apical sample point of long top leaders, the level of auxin was 450 times higher compared to short ones (Table 1). Contrary to auxin, the levels of cytokinins were highest in the apical sample point compared to the basal sample point (280% and 745% for short and long top leaders, respectively). Although the actual level of auxin and cytokinin varied considerable between short and long top leaders (Table 1) the auxin/cytokinin ratio remained low in the apical sample point independent of the length of the top leader (2.7 and 3.72 in short and long top leaders, respectively). In the basal sample point of short as well long top leaders, the ratio had increased nearly by a factor 10 (21.5 and 39.4, respectively, Table 1).

When plotting the individual cell lengths, it became evident that the variation is much smaller in short top leaders (25–75 µm) than in long ones (50–270 µm) (Fig. 6). In sector 1, the epidermis Feret diameter increases exponentially ($R^2 = 0.9994$) with the length of the shoot, indicating that increased cell length is a major cause of the final size of the top leaders. This difference caused the Fibonacci number to decrease from about 14 to 8. In top leaders treated with auxin (Pomoxon®), the commercial growth regulator in Christmas trees, the Feret diameter decreased equally at the top and basal sample point by about 1/3 and caused the distance between the rows of needle to become equal at the top and basal sample point (Table 3). However, the Fibonacci number was not influenced by the auxin treatment (Table 3).

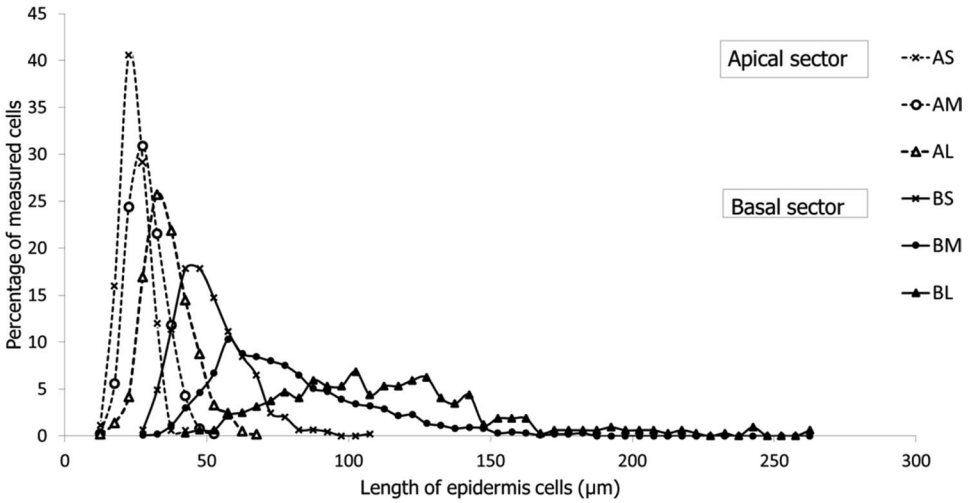

Fig. 6 Distribution of cell sizes within the stem epidermis layer of *A. nordmanniana* top leaders of different length. The measurements are made as Feret diameter. Dotted lines show the apical sector and solid lines show the basal sector. S: short top leaders (90 mm, times), M: medium top leaders (130 mm, open circle), L: long top leaders (270 mm, filled triangle). A: sample point 1 within the apical sector, B: sample point 5 within the basal sector

Table 1 Level of auxin and cytokinins in top leaders of *A. nordmanniana*

Top leader length (mm)	Sample point	IAA (pmol g FW^{-1})	Cytokinins (pmol g FW^{-1})	IAA/cytokinin ratio
90	1 (apical)	310[a]	114[a]	2.70
90	5 (basal)	860[b]	40[b]	21.5
270	1 (apical)	1404[c]	380[c]	3.72
270	5 (basal)	2011[c]	51[b]	39.4

Five top leaders of 90 mm and 270 mm were harvested July 15, 2015. From each size group, 10-mm stem sections from sample point 1 and 5 were analyzed for content of IAA and cytokinins (sum of *t*-zeatin, *t*-zeatinriboside, *t*-zeatinriboside-*O*-glucoside, dihydrozeatin and isopentanyladenine). Different letters indicate significant differences by Student's t test

Table 2 Morphological characterization of top leaders at the end of the growing season (September 1, 2014)

Sample point	Untreated top leaders	
	Distance between two rows of needles, mm	Fibonacci number
1	14.6 ± 3.1	7.3 ± 1.3
2	17.5 ± 6.5	8.7 ± 2.6
3	14.9 ± 4.0	12.4 ± 3.5
4	11.3 ± 2.9	13.7 ± 2.9
5	8.7 ± 2.9	13.8 ± 8.8

For sample points, see Fig. 1. Data are means of 20 measurements on five different top leaders and given as means ± SD

Discussion

Control of top leader elongation is of high importance for the commercial Christmas tree (*A. nordmanniana*) production. However, our understanding of the developmental changes that occur during top leader elongation in conifers lags behind our understanding of these processes in angiosperms. The Christmas tree, *A. nordmanniana*, has determined annual shoot growth. The growth capacity of the top leader is determined during bud developed the previous season by the number of stem units being initiated. The annual growth is thus restrained by the number of stem units being present within the shoot initial at the time of bud burst. However, in *Picea abies* it has been shown that the growth of the shoot initial depends on elongation of individual cells within each stem unit as well as additional cell divisions (Hejnowicz and Obarska 1995). Our study supports this finding, but reveals that the pattern of cell division and elongation differ between the base and top of the top leader. The fastest growth rate of the total top leader (21.6 mm/day) was observed mid-July. It was only the upper two-thirds of the top leader that was responsible for this rapid growth. The steep change in the growth curve for the middle section (Fig. 2) indicates that mainly cell elongation of the stem units is the cause of this rapid stem elongation. After mid-July, growth mainly occurs in the upper apical sector where a more stable growth rate indicates that a combination of cell division and elongation occurs (Table 2). The bell-shaped growth curve of the entire top leader accordingly had a pronounced right shoulder caused by a 4 weeks longer growth period in the apical sector compared to the basal and middle sectors (Fig. 2). This longer growth period is probably sustained by a high level of cytokinins present in the SAM in the last part of the top leader elongation period (Rasmussen et al. 2010). Furthermore, it is during this period of growth that the Fibonacci number is halved from about 14 to 7 in the upper 2 sample points (Table 2). All needles appear immediately after bud break, where the spiral arrangement can be observed (Fig. 1A, B). The observed change in the spiral composition in the upper two sample points, and therefore the Fibonacci

Table 3 Effect of NAA on epidermis cell size and morphology of top leaders

Sample point	NAA-treated top leaders		
	Decreased Feret diameter (%) (compared to control)	Distance between two rows of needles, mm	Fibonacci number
1	39.9 ± 5.1	8.7 ± 0.4 (control 14.6 ± 3.1)	8.8 ± 0.3 (control 7.3 ± 1.3)
5	31.8 ± 2.5	8.8 ± 1.7 (control 8.7 ± 2.9)	12.3 ± 3.0 (control 13.8 ± 8.8)

For sample points, see Fig. 1. Data are mean of three individual plants, and the diameters are mean of 100 cells ± SD

number may be a consequence of new meristematic activity initiated in the upper two sample points within the existing stem units. This has caused the rate of cell division and maturation time to differ from the processes that occurred in the developing bud the previous year during bud initiation in the fall.

In Nordmann fir, the level of auxin varies considerably during the elongation period of the top leader. In mid-July, the auxin level peaks at about 900 pmol g FW^{-1} in the middle sector of the top leader (Rasmussen et al. 2010), corresponding to the period of maximal daily growth in this sector (Fig. 2). The auxin needed for stem unit elongation most likely originates from the developing needles, as the level of auxin in the terminal bud is below detection limit during the period where the top leader elongates (Rasmussen et al. 2010). The alteration in the auxin/cytokinin ratio we have determined between the bud and stem (Veierskov 2018, Table 1) is most likely the cause of the variation in the rate of cell division and maturation that resulted in the observed changed Fibonacci number.

As it is the epidermal cells that restrict stem elongation, we have measured the Feret diameter of the epidermal cells. Even though the Feret diameter is not a direct volume estimate, we consider it a relevant measure for comparing cell elongation in different tissues. Cells in the apical sectors were shorter and more isodiametric than at the base regardless of top leader length (Figs. 3, 5). Epidermal cell anisotropy and size increased toward the basal sector (Figs. 3, 5) where cells had a more undulating contour (Figs. 3d, 4a).

The presence of the longest epidermal cells in the basal sector (Figs. 3, 5, 6) might thus be caused by the high level of auxin during the early elongation phase, as the growth of this sector mainly occurs until the top leader has reached 40% of its final length (Figs. 1, 2). The smaller cells (Figs. 3, 5, 6) and the increased distance between needles towards the apical meristem (Table 2) also correspond to the altered auxin/cytokinin ratio observed in the apical part of the top leader compared to the basal part (Table 1) as a high cytokinin level stimulates cell division (Veierskov 2018; Werner et al. 2001), whereas the low auxin levels diminish the ability of the cells to elongate.

In conifers, it has been described that the Fibonacci number may change in an elongating shoot due to an increased elongation of the stem units (Cannell and Bowler 1978). However, this experiment showed that the application of the auxin NAA decreases the Feret diameter by one-third, and thereby the distance between the needles, but without affecting the Fibonacci number (Table 3). This shows that the decreased Fibonacci number in the apical sector is not caused solely by increased cell elongation, but by de novo cell division and elongation in the existing stem units which having an altered maturation time. Further, it indicates that mode of action of NAA is on the process of cell elongation rather than cell division.

When epidermal peels from short (90 mm), medium (130 mm) or long (370 mm) top leaders were compared, the epidermis cells were longest at the base of the top leader, independently of its growth capacity. At the same time, the average cell length in this sector reflected the growth capacity and the auxin level in the leader. In the basal sector of a short top leader, cell length was less than half of that determined in a long top leader (25 vs. 110, Fig. 6).

Conclusion

Our data on the course of top leader growth show that the daily growth rate of all sections peaked at the time when the top leader had reached 40% of its final length. The basal sector contained the longest cells although the daily growth rate and needle distance were low here (Fig. 2), indicating a low rate of cell divisions, supported by a high auxin/cytokinin ratio. In the apical region, long distance between the needles and the shortest cells indicates a high rate of cell divisions in the stem units, sustained by a low auxin/cytokinin ratio. As the application of auxin to the top leaders also caused the needle distance to decrease, we conclude that in *A. nordmanniana* the auxin/cytokinin ratio controls stem unit elongation by regulating cell elongation as well as cell division. Contrary to angiosperms, where the phyllotaxi occurs in a continual self-organizing progression generated by the strict hormonal control of organ and tissue development within the meristem during shoot growth (Cannell and Bowler 1978; Jonsson et al. 2006; Murray et al. 2012; Reinhardt et al. 2003). The changes in the phyllotaxi in *A.*

nordmanniana are probably due to cell division and elongation within the stem units during the last part of top leader elongation. Furthermore, the growth of the top leader of Nordmann fir occurs by a gradual, basipetal elongation as in angiosperms. We expect that our observations are reflecting growth and development in related genera having buds with preformed shoot initials.

Acknowledgements The authors want to thank Professor Alexander Schulz for critical review of the manuscript and Sif Veierskov for providing the pictures of the top leaders.

Author Contributions SS was responsible for the field measurements, MB for the hormone determinations, and HM and BV contributed equally to the manuscript.

Funding This project was supported by a grant from the Danish Agricultural Agency (Grant 34009-15-0964) to B. Veierskov and the Danish National Research Foundation (Grant No. DNRF99) to M. Burow.

Compliance with Ethical Standards

Conflict of interest The authors declare no conflict of interest.

References

Baxter SM, Cannell MGR (1978) Branch development on leaders of picea-sitchensis. Can J For Res 8(1):121–128. https://doi.org/10.1139/x78-020

Boman BM, Dinh TN, Decker K, Emerick B, Raymond C, Schleiniger G (2017) Why do fibonacci numbers appear in patterns of growth in nature? A model for tissue renewal based on asymmetric cell division. Fibonacci Q 55(5):30–41

Brousseau A (1969) Fibonacci statistics in conifers. Fibonacci Q 7:7

Cannell MGR, Bowler KC (1978) Phyllotactic arrangements of needles on elongating conifer shoots—computer-simulation. Can J For Res 8(1):138–141. https://doi.org/10.1139/x78-022

Chen HJ, Bollmark M, Eliasson L (1996) Evidence that cytokinin controls bud size and branch form in Norway spruce. Physiol Plant 98(3):612–618

Hejnowicz A, Obarska E (1995) Structure and development of vegetative buds, from the lower crown of *Picea abies*. Annales Des Sciences Forestieres 52(5):433–447. https://doi.org/10.1051/forest:19950504

Jonsson H, Heisler MG, Shapiro BE, Meyerowitz EM, Mjolsness E (2006) An auxin-driven polarized transport model for phyllotaxis. Proc Natl Acad Sci USA 103(5):1633–1638. https://doi.org/10.1073/pnas.0509839103

Kutschera U, Nikas KJ (2007) The epidermal-growth-control theory of stem elongation: an old and a new perspective. J Plant Physiol 164(11):1395–1409. https://doi.org/10.1016/j.jplph.2007.08.002

Liesche J, Martens HJ, Schulz A (2011) Symplasmic transport and phloem loading in gymnosperm leaves. Protoplasma 248(1):181–190. https://doi.org/10.1007/s00709-010-0239-0

Maksymowych R, Orkwiszewski JAJ, Maksymowych AB (1989) Regions of cell-division and elongation during stem growth of xanthium. Am J Bot 76(10):1556–1558. https://doi.org/10.2307/2444444

Murray JAH, Jones A, Godin C, Traas J (2012) Systems analysis of shoot apical meristem growth and development: integrating hormonal and mechanical signaling. Plant Cell 24(10):3907–3919. https://doi.org/10.1105/tpc.112.102194

Powikrowska M, Oetke S, Jensen PE, Krupinska K (2014) Dynamic composition, shaping and organization of plastid nucleoids. Front Plant Sci 5:424. https://doi.org/10.3389/fpls.2014.00424

Rasmussen HN, Soerensen S, Andersen L (2003) Bud set in *Abies nordmanniana* Spach. influenced by bud and branch manipulations. Trees Struct Funct 17(6):510–514. https://doi.org/10.1007/s00468-003-0268-9

Rasmussen HN, Veierskov B, Hansen-Moller J, Norbaek R, Nielsen UB (2009) Cytokinin profiles in the conifer Tree *Abies nordmanniana*: whole-plant relations in year-round perspective. J Plant Growth Regul 28(2):154–166

Rasmussen HN, Veierskov B, Hansen-Moller J, Norbaek R (2010) "Lateral control": phytohormone relations in the conifer treetop and the short- and long-term effects of bud excision in *Abies nordmanniana*. J Plant Growth Regul 29(3):268–279. https://doi.org/10.1007/s00344-009-9132-5

Reinhardt D, Pesce ER, Stieger P, Mandel T, Baltensperger K, Bennett M, Traas J, Friml J, Kuhlemeier C (2003) Regulation of phyllotaxis by polar auxin transport. Nature 426(6964):255–260. https://doi.org/10.1038/nature02081

Rutledge ME, Frampton J, Blank G, Hinesley LE (2009) Naphthaleneacetic acid reduces leader growth of fraser fir christmas trees. Hortscience 44(2):345–348

Savaldi-Goldstein S, Peto C, Chory J (2007) The epidermis both drives and restricts plant shoot growth. Nature 446(7132):199–202. https://doi.org/10.1038/nature05618

Sutinen S, Partanen J, Vihera-Aarnio A, Hakkinen R (2009) Anatomy and morphology in developing vegetative buds on detached Norway spruce branches in controlled conditions before bud burst. Tree Physiol 29(11):1457–1465. https://doi.org/10.1093/treephys/tpp078

Tillman-Sutela E, Kauppi A (2000) Structures contributing to the completion of conifer seed germination. Trees Struct Funct 14(4):191–197. https://doi.org/10.1007/s004689900027

Veierskov B (2018) Auxin: cytokinine ratio may determine plant stem elongation. Arch Appl Sci Res AASR-101 https://doi.org/10.29011/AASR-101.100001

Veierskov B, Rasmussen HN, Eriksen B (2008) Ontogeny in terminal buds of *Abies nordmanniana* (Pinaceae) characterized by ubiquitin. Am J Bot 95(6):766–771. https://doi.org/10.3732/ajb.2007314

Werner T, Motyka V, Strnad M, Schmulling T (2001) Regulation of plant growth by cytokinin. Proc Natl Acad Sci USA 98(18):10487–10492. https://doi.org/10.1073/pnas.171304098

Willis L, Refahi Y, Wightman R, Landrein B, Teles J, Huang KC, Meyerowitz EM, Jönsson H (2016) Cell size and growth regulation in the *Arabidopsis thaliana* apical stem cell niche. Proc Nat Acad Sci 113(51):E8238–E8246

Zadnikova P, Simon R (2014) How boundaries control plant development. Curr Opin Plant Biol 17:116–125. https://doi.org/10.1016/j.pbi.2013.11.013